ORIGINAL ARTICLE



Mouse lipogenic proteins promote the co-accumulation of triacylglycerols and sesquiterpenes in plant cells

Yingqi Cai¹ · Payton Whitehead¹ · Joe Chappell² · Kent D. Chapman¹

Received: 30 October 2018 / Accepted: 22 March 2019 / Published online: 27 March 2019 © Springer-Verlag GmbH Germany, part of Springer Nature 2019

Abstract

Main conclusion Mouse FIT2 protein redirects the cytoplasmic terpene biosynthetic machinery to lipid-droplet-forming domains in the ER and this relocalization supports the efficient compartmentalization and accumulation of sesquiterpenes in plant cells.

Mouse (*Mus musculus*) fat storage-inducing transmembrane protein 2 (MmFIT2), an endoplasmic reticulum (ER)-resident protein with an important role in lipid droplet (LD) biogenesis in mammals, can function in plant cells to promote neutral lipid compartmentalization. Surprisingly, in affinity capture experiments, the *Nicotiana benthamiana* 5-epi-aristolochene synthase (NbEAS), a soluble cytoplasm-localized sesquiterpene synthase, was one of the most abundant proteins that coprecipitated with GFP-tagged MmFIT2 in transient expression assays in *N. benthamiana* leaves. Consistent with results of pull-down experiments, the subcellular location of mCherry-tagged NbEAS was changed from the cytoplasm to the LD-forming domains in the ER, only when co-expressed with MmFIT2. Ectopic co-expression of NbEAS and MmFIT2 together with mouse diacylglycerol:acyl-CoA acyltransferase 2 (MmDGAT2) in *N. benthamiana* leaves substantially increased the numbers of cytoplasmic LDs and supported the accumulation of the sesquiterpenes, 5-epi-aristolochene and capsidiol, up to tenfold over levels elicited by *Agrobacterium* infection alone. Taken together, our results suggest that MmFIT2 recruits sesquiterpene synthetic machinery to ER subdomains involved in LD formation and that this process can enhance the efficiency of sesquiterpene biosynthesis and compartmentalization in plant cells. Further, MmFIT2 and MmDGAT2 represent cross-kingdom lipogenic protein factors that may be used to engineer terpene accumulation more broadly in the cytoplasm of plant vegetative tissues.

Keywords Terpenes · Sesquiterpene synthase · Lipid droplet · Endoplasmic reticulum

Introduction

Terpenes represent a large and diverse group of bioactive plant metabolites, many of which are recognized for their physiological and ecological functions as well as

Electronic supplementary material The online version of this article (https://doi.org/10.1007/s00425-019-03148-9) contains supplementary material, which is available to authorized users.

- Kent D. Chapman chapman@unt.edu
- Department of Biological Sciences, Biodiscovery Institute, University of North Texas, 1155 Union Circle #305220, Denton, TX 76203-5017, USA
- Plant Biology Program and Department of Pharmaceutical Sciences, University of Kentucky, Lexington, KY, USA

their industrial and medicinal applications (Bohlmann and Keeling 2008; Hasegawa et al. 2010; Kappers et al. 2005; Schwab et al. 2008). Terpenes are synthesized from isopentenyl diphosphate (IPP) and dimethylallyl diphosphate (DMAPP), the C_5 building blocks that can be produced via two independent pathways—(1) mevalonate (MVA) pathway that is conserved in all eukaryotes, and (2) methylerythritol phosphate (MEP) pathway that operates in prokaryotes and plants. In plants, the MVA pathway is present in the cytoplasm and devoted to sesquiterpene (C_{15}) and triterpene (C_{30}) production, while the MEP pathway is localized to plastids and is responsible for the biosynthesis of monoterpenes (C_{10}) and diterpenes (C_{20}) (Hemmerlin et al. 2003; Tholl and Lee 2011).

With a growing understanding of terpene biosynthetic pathways, a number of approaches have been devised



to engineer elevated amounts of selected terpenoids in diverse species ranging from microorganisms to higher plants (Lange and Ahkami 2013; Reiling et al. 2004; Ro et al. 2006; Takahashi et al. 2007; Zhuang and Chappell 2015). As the natural source for many terpenes, plants provide a renewable, and potentially economically attractive platform for the metabolic engineering of terpenes. Efforts have included the production of terpenes in heterologous plant species. For instance, the synthesis of botryococcene, a triterpene normally generated by the green alga Botryococcus braunii, has been successfully engineered into Nicotiana tabacum leaves and Arabidopsis seeds by introducing an avian farnesyl diphosphate synthase (FDPS) and two B. braunii botryococcene synthases, SSL-1 and SSL-3 (Jiang et al. 2016; Kempinski and Chappell 2018). In recent years, producing large quantities of non-polar lipids in vegetative organs of plants has become an attractive strategy to meet the growing demand for energy-dense biomass and for the production of high-value, lipid-soluble bio-based products (Pyc et al. 2017b; Xu and Shanklin 2016; Yurchenko et al. 2017). Substantial progress has been made to significantly increase the accumulation of various terpenes in plant leaves by engineering terpene biosynthesis into chloroplasts (Jiang et al. 2016; Kempinski et al. 2018; Wu et al. 2006). However, efforts to direct the accumulation of terpenes using isoprenoid precursors derived from the MVA pathway in the cytoplasm have met with less success in plant tissues. This may be due to an incomplete understanding of how metabolic flux through the MVA might be regulated, or some toxicity effect of terpene accumulation engineered into the cytoplasm.

As hydrophobic compounds, terpenes are usually stored in specialized cells and organs of plants, such as oil cells, glandular trichomes, and resin canals (Brown 2010; Geng et al. 2012; Lange 2015). Attempts to use some of these mechanisms have been made. Brückner and Tissier (2013) described transient expression systems for the secretion of terpene to the epicuticular surfaces in Nicotiana benthamiana and Sallaud et al. (2012) developed a strategy for doing so in trichomes. However, Wu et al. (2012), reported that over-expression of terpene biosynthetic machinery in trichomes resulted in adverse phenotypic consequences on general plant growth, seriously limiting this approach. Alternative approaches such as installing novel terpene production into the chloroplast compartment (Wu et al. 2006, 2012) to divert carbon from the MEP pathway have been more successful in terms of terpene accumulation amounts, and extended by the heterologous expression of synthetic hydrophobic droplet-forming proteins also targeted the chloroplast compartment (Zhao et al. 2018).

Interest in engineering terpene accumulation in the cytoplasmic compartment has remained high in part because of the continuous and robust flux of carbon through the MVA

pathway. However, concerns about the ability of the cells to sequester significant amounts of hydrophobic terpenes in the cytoplasmic compartment linger and the notion of engineering a subcellular compartment that could sequester hydrophobic terpenes within the aqueous cytoplasm remains untested. Lipid droplets (LDs) are subcellular organelles comprising a core of neutral lipids enclosed by a monolayer of phospholipids and decorated by LD coat proteins which might offer a solution to this outstanding question. LDs serve as compartments for the packaging of various types of neutral lipids including triacylglycerols (TAGs), steryl esters, carotenoids, rubber (a polyisoprenoid), and oxylipins (Murphy 2001; Pyc et al. 2017b; Shimada et al. 2014). An increasing understanding of LD biogenesis in plants has suggested several effective tools and strategies to support the accumulation of LDs in plant vegetative tissues (Cai et al. 2017; Pyc et al. 2017b; Vanhercke et al. 2014). While cytoplasmic LDs in plants are most often associated with TAG storage in seeds and pollen grains, LDs are found in all plant cell types, and may represent a cytoplasmic location for the efficient deposition and storage of greater amounts of hydrophobic terpenes throughout plant tissues.

LDs are believed to originate from the endoplasmic reticulum (ER), where neutral lipids like TAGs are synthesized and enriched between the two leaflets of the ER bilayer. These neutral lipid aggregates, referred to as a "lens"-like structure, can eventually grow into mature LDs that dissociate from the ER into the cytoplasm (Pyc et al. 2017b; Wilfling et al. 2014). One of the proteins that has been demonstrated to play an important role in LD biogenesis is the fat storage-inducing transmembrane protein 2 (FIT2). FIT2 is an integral ER membrane protein that binds to and sequesters TAGs, and thereby promotes the proliferation of LDs (Choudhary et al. 2015; Gross et al. 2010, 2011; Kadereit et al. 2008). Recent studies of LD biogenesis have suggested an important role for FIT2 in controlling LD emergence via the modulation of ER lipid composition (Choudhary et al. 2018). While no apparent homologue of FIT2 has been identified in plant kingdom, the mouse (*Mus musculus*) MmFIT2 appears to function to promote LD biogenesis in plant cells in a manner similar to that in mammalian cells (Cai et al. 2017; Chapman et al. 2012). When ectopically expressed in N. benthamiana leaf cells or N. tabacum Bright Yellow (BY)-2 suspension-cultured cells, the MmFIT2 localized to the ER and subdomains where TAG accumulation occurs (Cai et al. 2017). Indeed, expression of MmFIT2 significantly increased the number and size of LDs in plant vegetative tissues, and increased the neutral lipid content in leaves (Cai et al. 2017). This dramatic influence on LD accumulation by a cross-kingdom protein with no homologues in plants led us to speculate that FIT2 may represent a means to synergistically couple biosynthetic machinery with that associated with packaging of neutral lipids, thus creating



a novel mechanism to accumulate high levels of targeted chemistries.

To gain insight into the LD-biosynthetic machinery at the ER associated with MmFIT2, we used GFP-tagged MmFIT2 to pull-down the proteins in the vicinity of MmFIT2 in N. benthamiana leaves via a GFP-based affinity-capture. Besides the ER-localized proteins involved in lipid biosynthesis and ER morphology, proteins associated with terpene biosynthesis were found in notably high abundance in the MmFIT2 pull-downs, which suggested that terpenes could be partitioned into cytoplasmic LDs in plant vegetative tissues. We followed up with the most abundant of these, a terpene synthase, 5-epi-aristolochene synthase (EAS), which is responsible for the biosynthesis of the first intermediate in the sesquiterpene phytoalexin biosynthetic pathway to capsidiol (Maldonado-Bonilla et al. 2008; Vögeli et al. 1990). Our results indicate that NbEAS is re-localized in a MmFIT2-dependent manner from its normal cytoplasmic location to ER subdomains that are dedicated to neutral lipid accumulation and LD budding. Furthermore, enhancing neutral lipid compartmentalization by MmFIT2 or stimulating additional neutral lipid (i.e., TAGs) synthesis by mouse diacylglycerol:acyl-CoA acyltransferase 2 (MmDGAT2) dramatically elevated the content of sesquiterpenes (5-epiaristolochene and capsidiol) in N. benthamiana leaves. Collectively, these data demonstrate that MmFIT2 recruits sesquiterpene synthase to the LD-forming domains of the ER and that this mammalian lipogenic protein appears to be an effective, albeit unexpected, target for engineering novel cellular compartments for the accumulation of valuable terpenes in vegetative tissues of plants.

Materials and methods

Plant growth conditions and *Agrobacterium*-mediated transient expression in *N. benthamiana* leaves

Nicotiana benthamiana plants were grown in soil in a growth room at 28 °C under a 14/10 h light/dark cycle. Wild-type Arabidopsis thaliana (Columbia-0) seeds were germinated on agar plates containing half-strength MS media (Murashige and Skoog 1962) and 2-week-old seedlings were transferred into soil and grown in a growth room at 21 °C under a 16/8 h light/dark cycle with 50 μE/m²/s light intensity.

Plant expression plasmids containing desired genes were transformed into *Agrobacterium tumefaciens* (GV3101) using Bio-Rad electroporation system following the manufacturer's manual. Transformed *Agrobacterium* cells containing appropriate binary vectors were inoculated in LB broth and incubated at 28 °C with shaking at 250 rpm until

early stationary phase ($OD_{600} \sim 1.5$). Agrobacterium cells were then resuspended in infiltration buffer (5 mM MES, 5 mM MgSO₄, 100 μ M acetosyringone, pH 5.7) and incubated at 28 °C with shaking for 3 h. Each Agrobacterium culture was diluted 10 times with infiltration buffer in the final culture mixture for infiltration. The top three fully expanded leaves of 4-week-old *N. benthamiana* plants were used for Agrobacterium infiltration. The Tomato Bushy Stunt Virus *P19* was included in all transgene infiltrations to suppress post-transcriptional gene silencing (Petrie et al. 2010).

RNA extraction, reverse transcriptase (RT)-PCR and plasmid construction

Total RNA was extracted from flowers of wild-type Arabidopsis as well as Agrobacterium-infiltrated N. benthamiana leaves using the RNeasy Plant Mini Kit (Qiagen, Germantown, MD, USA) and following the manufacturer's protocol. PrimeScript One Step RT-PCR Kit (Takara, Mountain View, CA, USA) was used for N. benthamiana transgene expression analysis following the manufacturer's instructions. Primers used to amplify P19, MmFIT2, MmDGAT2, FDPS, NbEAS, and NbEF1 α were listed in Supplemental Table 1. The RT-PCR program was as follows: 42 °C for 20 min, 95 °C for 5 min, 35 amplification cycles (94 °C for 30 s, 55 °C for 30 s, 72 °C 90 s), and 72 °C for 7 min. For gene cloning, 1 µg of RNA was used to generate cDNA library using iScript Select cDNA Synthesis Kit (Bio-Rad, Hercules, CA, USA). The AtTPS21 (AGI accession no. AT5G23960) coding sequence was amplified from Arabidopsis flower cDNA (50 ng) using primers TPS21F and TPS21R. The N. benthamiana EAS (GenBank accession no. MH939184) coding sequence was amplified using cDNA generated from Agrobacterium-infiltrated N. benthamiana leaf tissue and primers NbEASF and NbEASR. The coding sequence of avian FDPS (GenBank accession no. P08836) was PCR amplified from plasmid pBDON-FPS-SSL1-3 (Jiang et al. 2016) using primers FDPSF and FDPSR. The mouse DGAT2 (GenBank accession no. BC043447) open reading frame was subcloned from pCMV6-MmDGAT2 construct (purchased from OriGene Global, Rockville, MD, USA) using primers DGAT2F and DGAT2R. The PCR reactions were performed using Phusion® DNA Polymerase (New England Biolabs, Ipswich, MA, USA) and the program was as follows, 98 °C for 2 min, 35 amplification cycles (98 °C for 10 s, 55 °C for 30 s, 72 °C 60 s), and 72 °C for 7 min. The sequences of primers used in this study are listed in Supplemental Table 1. The open reading frames of the genes described above were cloned into the plant binary vectors pMDC32 and/or pMDC32-mCherry using restriction enzymes AscI and PacI. The plasmids containing MmFIT2 were constructed previously (Cai et al. 2017).

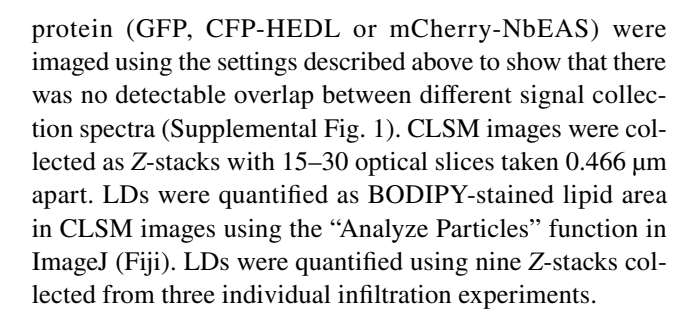


Affinity-capture assay and proteomics analysis

GFP-based affinity-capture assays were carried out using GFP-Trap[®] A (ChromoTek, Hauppauge, NY, USA). The detailed procedures for affinity-capture assay and proteomic analysis were described previously (Pyc et al. 2017a). Briefly, N. benthamiana leaves (approximately 1.5 g) transiently transformed with cDNAs encoding GFP alone or the GFP-MmFIT2 fusion were collected at 3 days post-Agrobacterium infiltration. Total proteins were extracted from the homogenized leaf tissue using 3 mL of extraction buffer [pH 7.5, 50 mM TRIS-HCl, 150 mM NaCl, 10% glycerol, 1% NP-40, 1 mM PMSF, 2 tablets of Roche protease inhibitor cocktail in 10 mL buffer (Sigma-Aldrich, St. Louis, MO, USA)] followed by centrifugation at 16,000g, 4 °C for 20 min. The supernatant was incubated with 30 µL of GFP-Trap®_A beads and the beads were then washed four times with extraction buffer. The proteins bound to beads were eluted with 100 µL of 4×SDS sample buffer and incubated at 70 °C for 10 min. The eluted protein samples were concentrated by electrophoresis allowing the protein sample to migrate just into the top (5-10 mm) of an SDS-PAGE gel (BoltTM 4–12%, Thermo Fisher Scientific, Grand Island, NY, USA). The gel was then stained with QC Colloidal Coomassie Stain (Bio-Rad, Hercules, CA, USA) and the concentrated protein bands were excised and submitted to the Michigan State University Proteomics Core Service (https ://rtsf.natsci.msu.edu/proteomics/) for proteomic analysis. Proteins in gel bands were treated with trypsin and purified peptides were analyzed using a Q-Exactive mass spectrometer (Thermo Fisher Scientific, Grand Island, NY, USA). The proteins were identified by searching the MS/MS spectra against the N. benthamiana protein database downloaded from the Sol Genomics Network (v.0.4.4; http://www.solge nomics.net).

Microscopy and LD quantification

Confocal fluorescence microscopy was performed using a Zeiss LSM 710 confocal laser-scanning microscope (CLSM). LDs in *N. benthamiana* leaves were stained with 2 µg/mL BODIPY 493/503 (4 mg/mL stock in DMSO, Invitrogen, Thermo Fisher Scientific, Grand Island, NY, USA) in 50 mM PIPES buffer (pH 7.0) for 30 min, followed by washing with 50 mM PIPES buffer (pH 7.0) three times and one time with deionized water. BODIPY 493/503 and GFP were excited by a 488-nm laser and emission signals were collected in a spectrum of 500–540 nm. CFP, mCherry and chlorophyll autofluorescence were excited with a laser at 405 nm, 561 nm and 633 nm, respectively. Emission signals of CFP, mCherry and chlorophyll were acquired from 450 to 490 nm, 590–640 nm and 640–720 nm, respectively. *N. benthamiana* leaf cells expressing single fluorescence



Analysis of neutral lipids

Approximately 50 mg of lyophilized N. benthamiana leaf tissue was used for lipid extraction in each biological replicate (n=3). Total lipids were extracted with isopropanol/ chloroform 2:1, followed by washing with 1 M KCl twice. A TAG (tri-15:0) standard (4 µg, Avanti Polar Lipids, Alabaster, AL, USA) was added to each sample for quantification. Detailed procedures for lipid extraction and purification were described previously (Cai et al. 2015). Solid-phase extraction (SPE) was performed to fractionate lipid extract based on polarity using Discovery® DSC-Si SPE Tube (Sigma-Aldrich, St. Louis, MO, USA), and the neutral lipid fraction was eluted with hexane/diethyl ether 4:1. The neutral lipid fraction was injected into electrospray ionization mass spectrometry (ESI-MS) combined with an API3000 triple quadrupole mass spectrometer (Applied Biosystems/ Sciex, Framingham, MA, USA), and TAGs were quantified using program Metabolite Imager (v.1.0, Horn and Chapman 2014).

Analysis of sesquiterpenes

For 5-epi-aristolochene extraction, approximately 500 mg fresh weight of N. benthamiana leaf tissue were collected and homogenized in liquid nitrogen (n=3). Homogenized tissue powder was transferred into a glass vial containing 2 mL of hexane and 100 ng of α-cedrene and incubated at room temperature on a rotation shaker (100 rpm) for 1 h and then 4 °C overnight. The residual tissue was lyophilized for measurement of dry weight. The hexane extract was purified by passing through the SPE cartridge (Discovery® DSC-Si, Sigma-Aldrich, St. Louis, MO, USA) and further eluted with 1 mL of hexane. Purified extract was transferred to a new glass vial placed on ice and concentrated slowly under a gentle stream of nitrogen to approximately 100 µL without drying down the sample completely. An aliquot (1 µL) of the concentrated extract was analyzed by gas chromatography-mass spectrometry (GC-MS) equipped with Agilent GC 7890A/MSD 5975C system and HP-5MS capillary column (30 m \times 0.250 mm, 0.25-mm coating thickness; Agilent Technologies, Santa Clara, CA, USA). The program of oven temperature was as follows, 70 °C for 1 min, 20 °C/min to 90 °C, 3 °C/min to



170 °C, 30 °C/min to 280 °C, 280 °C for 5 min, 20 °C/min to 300 °C, and 300 °C for 1 min. The inlet temperature was set at 250 °C, and ultrapure helium was used as the carrier gas with a constant flow of 0.5 mL/min. The mass spectra were first recorded under full mass scan mode to confirm the identity of α -cedrene and 5-epi-aristolochene (representative mass spectra shown in Supplemental Fig. 2). Then, 5-epi-aristolochene was quantified against α -cedrene using single-ion monitoring (SIM) mode (representative chromatograms shown in Supplemental Fig. 3). The fragment ion with a mass to charge ratio (m/z) 105 was used as the quantitative ion for both α -cedrene and 5-epi-aristolochene. The fragment ions with m/z 105, 119, 161, and 204 were used as diagnostic ions for α -cedrene, and the diagnostic ions for 5-epi-aristolochene were m/z 105, 161, 189, and 204.

Capsidiol was extracted from homogenized N. benthamiana leaf tissue (approximately 300 mg fresh weight) using 2 mL of chloroform shaking at room temperature for 1 h and then 4 °C overnight. The dry weight of the tissue was determined by measuring the remaining lyophilized tissue. The chloroform extract was then purified by SPE (Discovery® DSC-Si cartridge, Sigma-Aldrich, St. Louis, MO, USA), whereby leaf extract was loaded into the SPE column, washed with hexane/ diethyl ether 4:1 and hexane/diethyl ether 1:1, and eventually eluted with chloroform/methanol 1:2. Purified extract was derivatized by incubating with N,O-Bis(trimethylsilyl)trifluoroacetamide (BSTFA) at 50 °C for 1 h, and the derivatized sample was analyzed by the GC-MS described above. Derivatized capsidiol was quantified against α-cedrene under full mass scan mode (representative mass spectra and chromatograms shown in Supplemental Figs. 2 and 3). The oven temperature program was set as follows, 70 °C for 1 min, 20 °C/min to 90 °C, 8 °C/min to 250 °C, 30 °C/min to 280 °C, 280 °C for 5 min, 20 °C/min to 300 °C, and 300 °C for 1 min.

Statistical significance of the results

Three biological replicates were used for quantifications of LDs, TAGs and sesquiterpenes, and the significance analysis was performed using one-way ANOVA test followed by Tukey's post-test. The pull-down of terpene-related *N. benthamiana* proteins by MmFIT2 was reproducible in three communoprecipitation experiments. The subcellular localization phenotype is shown in Figs. 1, 2 and Supplemental Fig. 4 were observed in more than four leaves from at least two different infiltration experiments.

Results

Terpene-related proteins were identified as high abundance proteins that co-precipitate specifically with Mm FIT2

Studies of FIT2 in mammalian cells have suggested that the ER-localized FIT2 protein binds to TAGs within the ER bilayer and modulates ER lipid composition at LDforming sites to promote the proliferation of LDs (Choudhary et al. 2018; Gross et al. 2010, 2011; Kadereit et al. 2008). Our previous studies of ectopically expressing MmFIT2 in plants also demonstrated that MmFIT2 can function to induce LD accumulation in plant cells in a manner similar to that in mammalian cells (Cai et al. 2017). Despite the lack of an apparent homologue of MmFIT2 in plants, the functional conservation of MmFIT2 in promoting LD accumulation in plant cells prompted us to ask if MmFIT2 would interact with endogenous plant ER proteins involved in LD biogenesis. Toward that end, a GFP-tagged MmFIT2 was transiently expressed in N. benthamiana leaves, then GFP- MmFIT2 and its interacting proteins were affinity-captured using GFP-based immunoprecipitation system (GFP-TrapTM). As a control for specificity, N. benthamiana leaves expressing just GFP protein and no FIT2 fusion were analyzed to rule out proteins that were captured through non-specific interactions. The affinity-captured proteins were identified using mass spectrometric sequencing of enzyme-digested peptides (Shevchenko et al. 1996).

A total of 703 N. benthamiana endogenous proteins were recovered in the GFP-MmFIT2 pull-downs that were not detectable in the GFP-only control sample, including ER-localized proteins involved in lipid metabolism and ER membrane-shaping [i.e., lysophosphatidylcholine acyltransferase (LPCAT), glycerol-3-phosphate acyltransferase (GPAT), and reticulons] (see the complete list in Supplemental Table 2) (Li-Beisson et al. 2010; Sparkes et al. 2010). Intriguingly, these lipid- and ER-morphologyrelated proteins were of relatively low abundance in the MmFIT2 pull-down list, ranking from 259 to 594. However, more surprising was that amongst the most abundant of the co-purifying proteins were enzymes involved in terpene biosynthesis and accumulation (Table 1). The most abundant MmFIT2 pull-down protein, Pleiotropic Drug Resistance Protein 1 (PDR1), is an ATP-Binding Cassette (ABC) transporter involved in anti-pathogen terpenoid transport in N. tabacum and N. plumbaginifolia (Crouzet et al. 2013; Jasiński et al. 2001; Sasabe et al. 2002). Ectopic expression of the Artemisia annua PDR in N. benthamiana leaves enhanced the accumulation of artemisinin produced by co-expressed enzymes in the



artemisinin biosynthesis pathway (Wang et al. 2016). Other terpene-related, specifically captured proteins were enzymes catalyzing successive reactions in the capsidiol biosynthesis pathway, including FDPS, EAS and 5-epiaristolochene-1,3-dihydroxylase (EAH) (Table 1). EAS is a sesquiterpene synthase that catalyzes the cyclization of farnesyl diphosphate (FPP, produced by FDPS) into 5-epi-aristolochene, which is subsequently hydroxylated by the cytochrome P450 EAH enzyme to yield the di-hydroxylated sesquiterpene, capsidiol (Ralston et al. 2001; Starks et al. 1997; Tarshis et al. 1994; Vögeli et al. 1990). The terpene-related, co-purifying proteins PDR1, EAS, and FDPS were detected with high frequency, based on normalized spectral counts, which suggests that these proteins were significant components of the MmFIT2interacting complex (Table 1). It was curious that these terpene-related proteins would interact specifically with the ER-localized lipogenic protein MmFIT2, since PDR1, EAS, and FDPS do not localize to the ER normally. However, given the hydrophobicity of terpenoids, it is possible that the neutral lipids (i.e., TAGs) accumulated in the MmFIT2-induced LD-forming domain might serve as a hydrophobic co-solvent for terpenoids, which may support the re-localization of terpene-metabolizing enzymes near to the TAG-accumulating domains induced by MmFIT2. In any case, the co-purification of terpene-related proteins with MmFIT2 suggested that sesquiterpene accumulation could be impacted by the MmFIT2. As PDR is a large family with diverse functions and EAH is in low abundance in the pull-down, follow-up experiments were designed to test the co-localization of NbEAS and MmFIT2 in situ.

MmFIT2 re-localizes NbEAS from the cytoplasm to ER subdomains involved in lipid accumulation and LD formation

The abundant occurrence of *N. benthamiana* EAS protein found in the MmFIT2 pull-down sample suggests that NbEAS and MmFIT2 should be at least in proximity to each

other at the subcellular level. Given that EAS is a soluble cytoplasmic enzyme (Facchini and Chappell 1992), we hypothesized that NbEAS re-localized from cytoplasm to the ER in an MmFIT2-dependent manner. We, therefore, assessed the subcellular localization of NbEAS in transiently expressed N. benthamiana leaves via confocal fluorescence microscopy. A mCherry fluorescent protein was cloned inframe to the N-terminus of NbEAS and the fusion protein was transiently expressed in N. benthamiana leaves via Agrobacterium infiltration with or without co-expression with MmFIT2. mCherry-tagged NbEAS localized exclusively to the cytoplasm in the absence of MmFIT2 (Fig. 1a), indicated by the co-localization of mCherry-NbEAS with non-targeted GFP (a co-infiltrated cytoplasm marker). N. benthamiana mesophyll cells expressing MmFIT2 showed an altered ER morphology, indicated by ER marker (CFP-HDEL, Cai et al. 2015), whereby the reticulate ER network formed globular regions that were not observed in cells expressing the ER marker by itself (compare Fig. 1a, second row with Supplemental Fig. 1, second row). This ER phenotype is consistent with observations in our previous studies, where the MmFIT2-induced aggregated ER regions that were localized with neutral-lipid specific markers were suggested to be exaggerated ER subdomains responsible for TAG biosynthesis and LD formation (Cai et al. 2017). When co-expressed with MmFIT2, mCherry-tagged NbEAS was co-localized with the ER marker, exactly overlapping the globular regions induced by MmFIT2 (Fig. 1a). The significant influence of MmFIT2 on NbEAS subcellular localization suggests that MmFIT2 supports a re-localization of NbEAS from cytoplasm to the ER, and this is further supported by the co-localization of GFP-tagged MmFIT2 and mCherry-tagged NbEAS (Fig. 1b).

To further confirm that the MmFIT2-induced, NbEAS-accumulated globular ER regions are subdomains for LD biogenesis, the *N. benthamiana* leaves co-expressing MmFIT2, mCherry-NbEAS and the ER marker (CFP-HDEL) were stained with neutral lipid stain, BODIPY 495/503, and imaged with confocal fluorescence microscope

 Table 1
 List of terpene-related N. benthamiana proteins co-precipitated with GFP-MmFIT2

N. benthamiana accession no.	N. benthamiana protein name	Normalized spectra count		Ranking number	Arabidopsis
		Free GFP	GFP-MmFIT2	of abundance	homolog AGI no.
NbS00038999g0004	Pleiotropic drug resistance protein 1	0	40.53	1	AT1G15520
NbS00055581g0001	5-Epi-aristolochene synthase	0	22.19	5	AT5G23960
NbS00029252g0012	Farnesyl diphosphate synthase	0	17.37	11	AT4G17190
NbS00006716g0007	5-Epi-aristolochene-1,3-dihydroxylase	0	0.96	497	AT3G26300

The names and accession numbers of *N. benthamiana* proteins were acquired from *N. benthamiana* genome database downloaded from the Sol Genomics Network (www.solgenomics.net, v0.4.4). Normalized spectra counts represent quantities of co-precipitated proteins. The ranking number of abundance indicates relative abundance of each protein in the entire pull-down list (Supplemental Table 2). The *Arabidopsis* homolog AGI numbers are available at the *Arabidopsis* information resource (TAIR) database (www.arabidopsis.org)



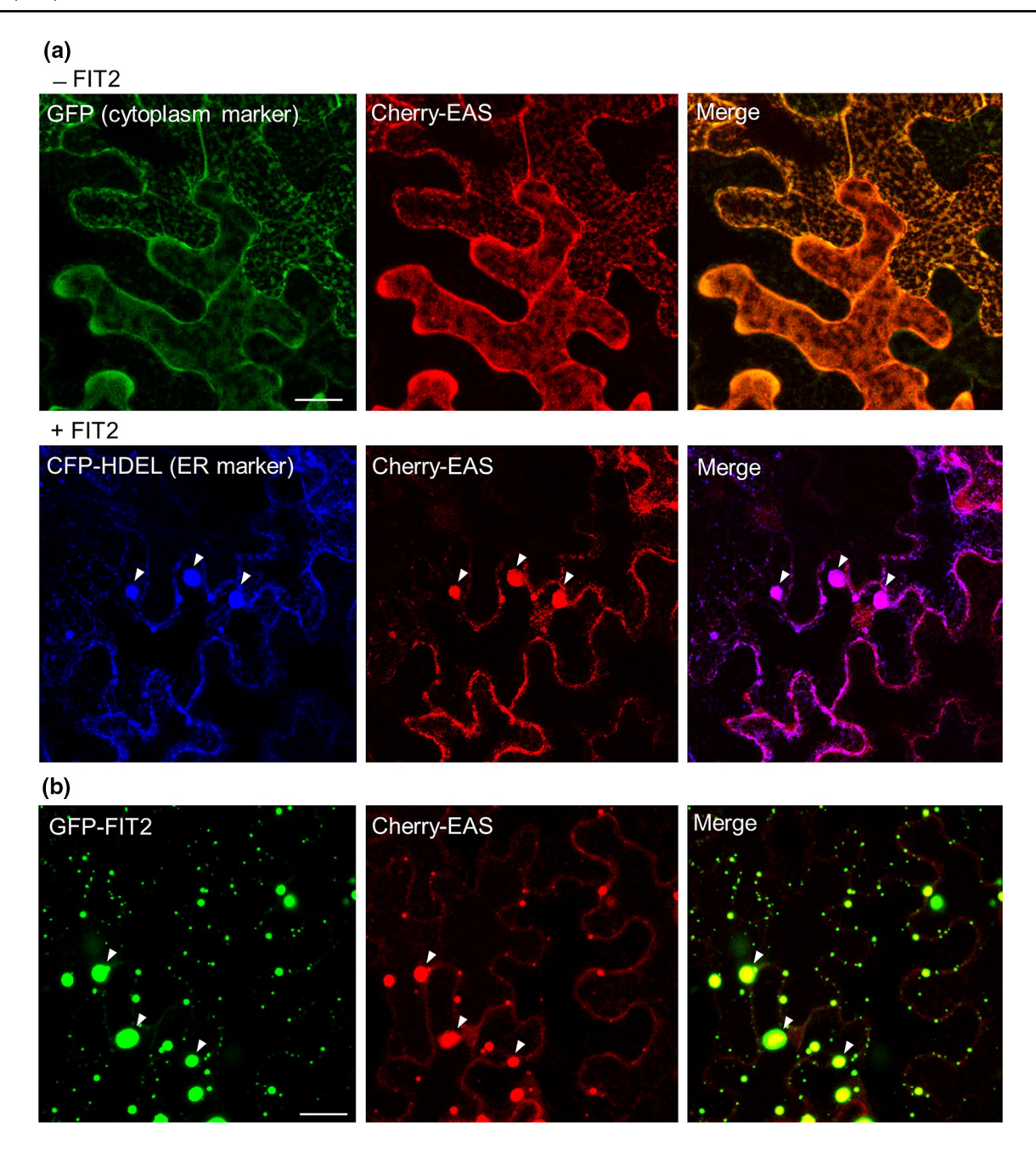


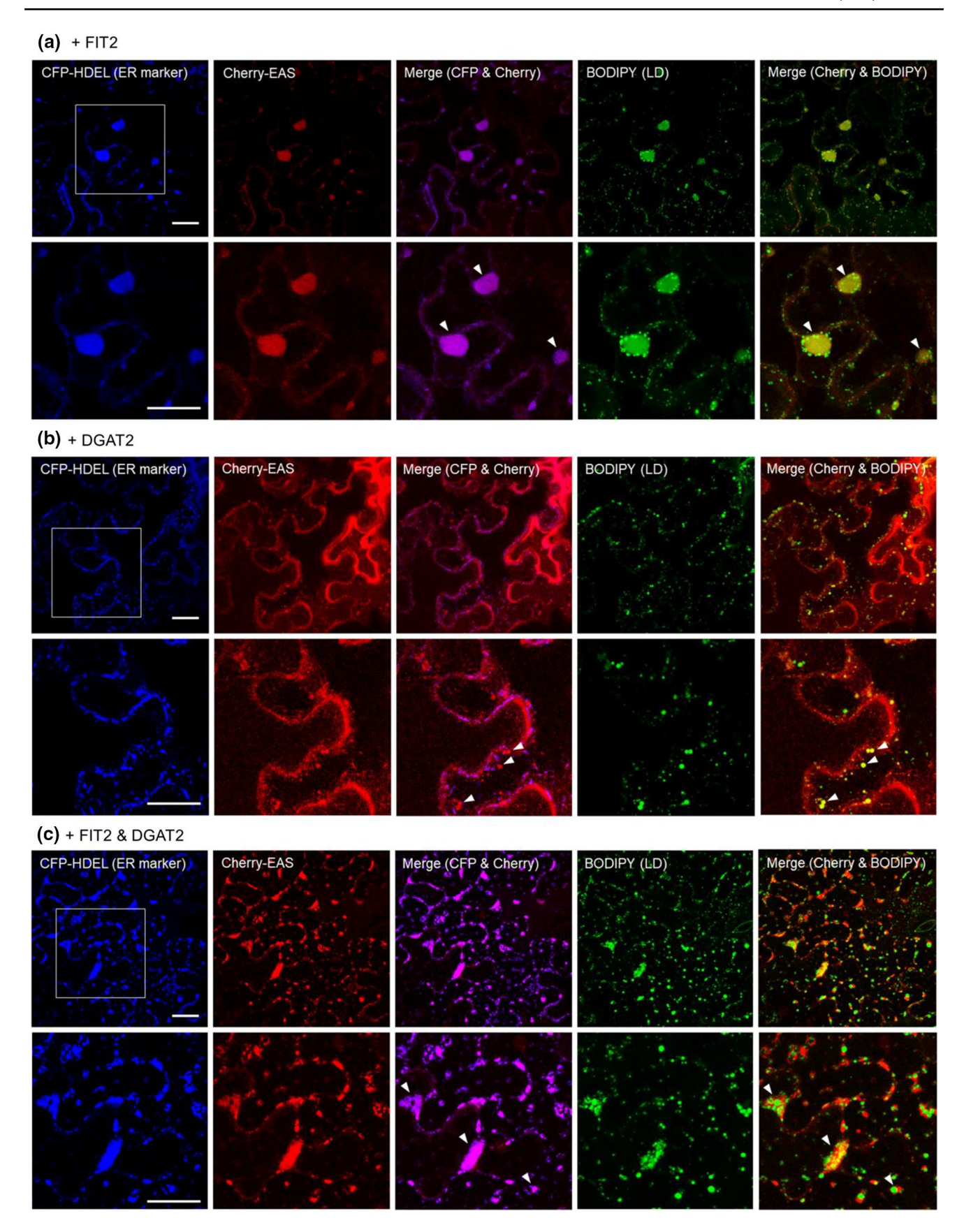
Fig. 1 MmFIT2 expression changes the subcellular location of NbEAS from the cytoplasm to the ER. **a** Confocal microscopic images of *N. benthamiana* leaf cells expressing mCherry-tagged NbEAS and organelle markers with or without co-expression of MmFIT2. The subcellular locations of NbEAS, cytoplasm, and ER were defined based on the fluorescence signals of mCherry-NbEAS (red), free GFP (green), and CFP-HDEL (blue), respectively. In the merged images, co-localizations of mCherry-NbEAS and the cytoplasmic marker as well as mCherry-NbEAS and ER marker are

shown in yellow and magenta, respectively. Arrowheads in the second row indicate representative regions of ER overlapping with mCherry-NbEAS. Images are projections of Z-stacks with 15–20 slices taken 0.466 μm apart within the abaxial surface of the leaf. Bar 20 μm. **b** Co-localization of GFP-MmFIT2 and mCherry-NbEAS in *N. benthamiana* leaves. GFP-MmFIT2, mCherry-NbEAS, and co-localizations are shown in green, red, and yellow, respectively. Arrowheads indicate apparent co-localizations of GFP-MmFIT2 and mCherry-NbEAS. Images were collected as describe in **a**. Bar 20 μm

to visualize the subcellular distribution of neutral lipids. Indeed, in the presence of MmFIT2, the mCherry-NbEAS was re-localized to CFP-labeled ER, and these structures were concentrated at the MmFIT2-induced spherical ER

regions where the BODIPY fluorescence signal was detected along with numerous small-sized LDs (Fig. 2a), suggesting that these ER regions were ER subdomains for neutral lipid accumulation and LD formation.







▼Fig. 2 Subcellular locations of NbEAS, ER, and LDs in N. benthamiana leaves in the presence of MmFIT2 and/or MmDGAT2. Shown are confocal images of BODIPY (493/503)-stained N. benthamiana leaf cells expressing mCherry-NbEAS and the ER marker with coexpression of MmFIT2 (a), MmDGAT2 (b), or both MmFIT2 and MmDGAT2 (c). NbEAS, ER, and LDs were visualized based on the fluorescence patterns of mCherry-NbEAS (red), CFP-HDEL (blue), and BODIPY (green), respectively. Co-localizations of ER and mCherry-NbEAS as well as LDs and mCherry-NbEAS are shown in magenta and yellow, respectively, in the corresponding merged images. Arrowheads indicate example regions of mCherry-NbEAS overlapping with ER and/or LDs. Images in the second row of each panel are approximately twofold magnifications of images in the first row indicated by box frames. Bar 20 μm

We then asked if NbEAS would localize to any hydrophobic compartments that contained neutral lipids. The cDNA sequence encoding MmDGAT2, the enzyme catalyzes the last step of TAG biosynthesis (Yen et al. 2008), was included in Agrobacterium infiltrations to increase TAG production and promote LD accumulation in N. benthamiana leaves by a mechanism independent of MmFIT2. As shown in Fig. 2b, the ER in cells expressing MmDGAT2 appeared to be a normal, reticulate network, and the fluorescence pattern of mCherry-NbEAS did not overlap with CFP-indicated ER. While mCherry-NbEAS occasionally overlapped with or was in proximity to cytoplasmic LDs induced by MmDGAT2, the majority of mCherry-NbEAS remained in the cytoplasm (Fig. 2b). In other words, inducing LD accumulation on its own did not efficiently re-localize NbEAS from cytoplasm to LDs. When MmFIT2 and MmDGAT2 were co-expressed in N. benthamiana leaves, ER was reoriented into discrete regions associated with many LDs, indicating that co-expression of MmFIT2 and MmDGAT2 reorganized ER into domains devoted to LD biogenesis (Fig. 2c). The co-expressed mCherry-NbEAS was almost exclusively localized to these ER "MmFIT2-induced domains" (Fig. 2c). Notably, while the cytoplasmic LDs in cells expressing both MmFIT2 and MmDGAT2 seemed to be larger and more abundant than those in cells expressing MmFIT2 or MmDGAT2 alone, no apparent co-localization of mCherry-NbEAS and cytoplasmic LDs was observed with coexpression of MmFIT2 and MmDGAT2 (Fig. 2c), suggesting that MmFIT2 plays a distinct role in recruiting NbEAS to LDforming domains of ER. Collectively, these subcellular localization data suggest that the NbEAS protein tends to localize to the hydrophobic ER subcompartments induced by MmFIT2 and to a lesser extent to the LDs induced by MmDGAT2. However, it seems that MmFIT2 can support the retention of NbEAS in ER subdomains actively engaged in LD biogenesis.

We next tested whether MmFIT2 could support the relocalization of sesquiterpene synthases other than NbEAS. The *Arabidopsis* homologue of *N. benthamiana* EAS, terpene synthase 21 (AtTPS21), is a sesquiterpene synthase catalyzing the conversion of FPP to beta-caryophyllene and alphahumulene (Tholl and Lee 2011). As shown in Supplemental

Fig. 4, AtTPS21 localized to the cytoplasm in the absence of MmFIT2, as indicated by the co-localization of mCherry-AtTPS21 with non-targeted GFP. Similar to NbEAS, when co-expressed with MmFIT2, the mCherry-tagged AtTPS21 was localized to the ER (indicated by CFP-HDEL), and accumulated at the globular ER regions (Supplemental Fig. 4). In addition, mCherry-AtTPS21 co-localized with GFP-MmFIT2 when co-expressed in *N. benthamiana* leaves (Supplemental Fig. 4). To test whether expression of MmFIT2 would result in redistribution of any random protein, we co-expressed GFP-MmFIT2 with untagged mCherry in N. benthamiana leaves. Confocal images of transformed N. benthamiana leaf cells (Supplemental Fig. 5) showed no overlap of GFP-MmFIT2 and mCherry fluorescence signal, suggesting that the subcellular localization of untagged mCherry was not influenced by MmFIT2 expression. These observations suggest that the MmFIT2-induced re-localization is not limited to NbEAS, and that MmFIT2 may be used to recruit sesquiterpene synthases of various types for the engineering of a wide array of specialty terpenes.

Expression of MmFIT2 and MmDGAT2 in *N. benthamiana* leaves results in increased accumulation of TAGs and sesquiterpenes

The significant influence of MmFIT2 on NbEAS subcellular distribution and proximity to neutral lipid domains of the ER further supported the premise that MmFIT2 might also support enhanced or elevated sesquiterpene accumulation in plant cells. The hydrophobicity of sesquiterpenes as well as the localization of NbEAS to hydrophobic cell compartments suggest that the content of neutral lipids may also be important for sesquiterpene accumulation. We, therefore, evaluated the effects of MmFIT2 and MmDGAT2 on the accumulation of LDs, TAGs, and sesquiterpenes in N. benthamiana leaves. It was previously demonstrated that MmFIT2 is primarily involved in promoting LD proliferation rather than directly inducing the biosynthesis of neutral lipids, and by increasing the efficiency of lipid partitioning, MmFIT2 can further enhance the accumulation of neutral lipids induced by proteins involved in lipid biosynthesis (Cai et al. 2017; Pyc et al. 2017b). Following this scenario, we transiently expressed MmFIT2 and MmDGAT2 individually and in combination in N. benthamiana leaves and examined their influence on the accumulation of LDs and TAGs (Fig. 3). As shown in the confocal microscopic images of BODIPY-stained *N. benthamiana* mesophyll cells, leaves expressing MmFIT2 accumulated more LDs compared to the mock (infiltration buffer only) or P19 (viral protein P19 only) controls, which produced very few LDs (Fig. 3a). In addition, expression of MmDGAT2 by itself and in combination with MmFIT2 appeared to produce more LDs than MmFIT2 alone (Fig. 3a). These observations were further



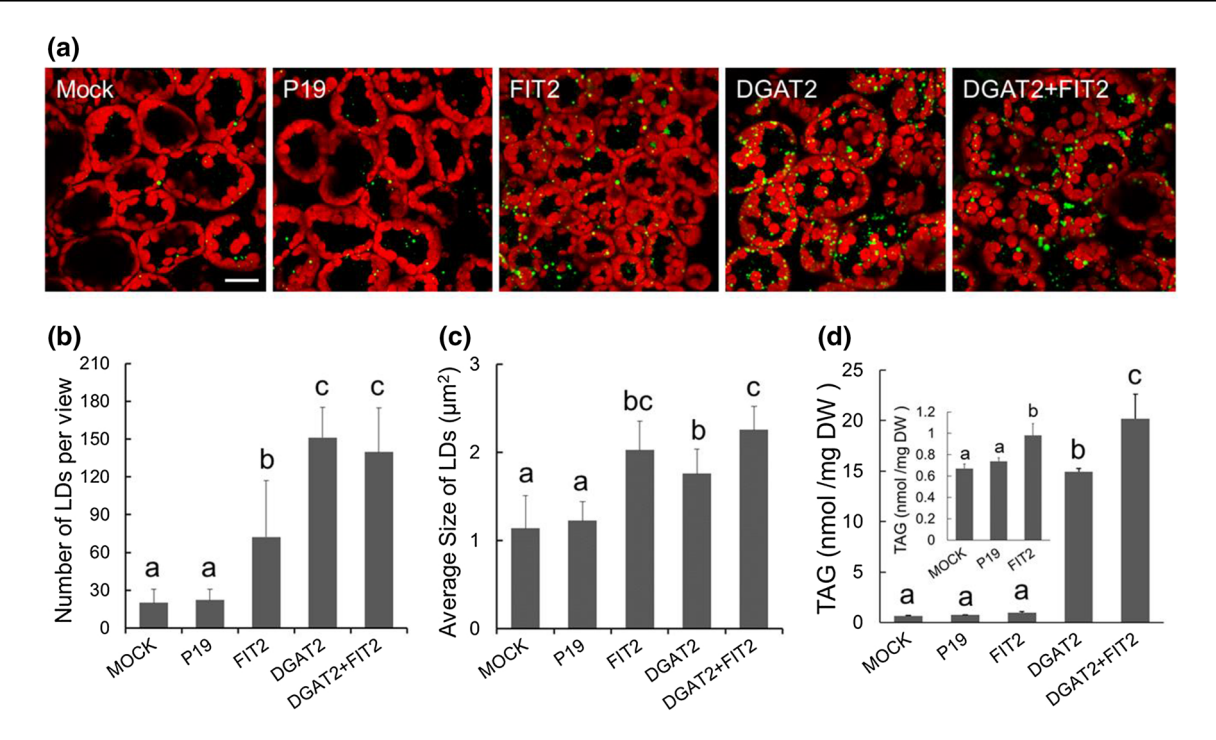


Fig. 3 Expression of MmFIT2 and MmDGAT2 promotes proliferation of LDs and elevates the contents of triacylglycerols (TAGs) in *N. benthamiana* leaves. **a** Representative confocal microscopic images of BODIPY (493/503)-stained *N. benthamiana* leaves expressing MmFIT2, MmDGAT2, or both MmFIT2 and MmDGAT2. LDs were visualized based on the fluorescence signal of the neutral lipid stain BODIPY (green). Red color represents chloroplast autofluorescence. Mock treatment was infiltration with buffer only. The viral suppressor protein P19 was infiltrated by itself as a negative control and was included in all the infiltrations with transgenes. Images are

projections of Z-stacks consisting of 30 slices taken 0.466 μ m apart within the mesophyll. Bar 20 μ m. **b**-**d** Show quantifications of LD number, LD size, and triacylglycerol content, respectively. LD number and size were quantified using ImageJ as BODIPY-stained areas in Z-stack projections. Values of LD number and size are averages and SD of nine Z-stacks collected from three individual infiltrations. Values of triacylglycerol content are averages and SD of four biological replicates. Different letters on top of bars indicate significant difference at P<0.05 determined by one-way ANOVA followed by Tukey's post-test

confirmed by the quantification of LD number and size, which indicated that both the numbers and the average size of LD were greatly increased when MmFIT2 was present (Fig. 3b, c). Despite the marked increase of LD number and size induced by MmFIT2, the content of TAGs in N. benthamiana leaves transformed with MmFIT2 alone was only increased by ~40% over the P19 control (Fig. 3d). By contrast, MmDGAT2 produced over 20 times more TAGs compared to that in the control leaves (Fig. 3d). Further, MmFIT2 in cooperation with MmDGAT2 led to a ~ 28-fold increase in TAG content in N. benthamiana leaves compared with the mock and P19 controls (Fig. 3d). These data are consistent with the concept that MmFIT2 does not directly participate in neutral lipid biosynthesis but rather supports more efficient packaging of neutral lipids into cytoplasmic LDs, while MmDGAT2 can directly stimulate the biosynthesis of TAGs.

We next quantified the contents of two sesquiterpenes (1) 5-epi-aristolochene, the direct product of NbEAS, as well as (2) capsidiol, the product of subsequent hydroxylation of 5-epi-aristolochene in *N. benthamiana* leaves. As shown

in Fig. 4, despite the similar trends of increased amounts of both 5-epi-aristolochene and capsidiol in transgenic leaves, the amounts of 5-epi-aristolochene were substantially lower than capsidiol in all leaf samples, which was expected since 5-epi-aristolochene is an intermediate metabolite in the synthesis of capsidiol in tobacco leaves (Whitehead et al. 1989). 5-Epi-aristolochene is also volatile and some could be lost to evaporation. No 5-epi-aristolochene or capsidiol were detected in the leaves infiltrated with buffer only (mock). Detectable amounts of both 5-epi-aristolochene and capsidiol were found in leaves transformed with Agrobacterium containing P19 alone (Fig. 4), and this is expected since Agrobacterium infection like other pathogen elicitors stimulates the production of these sesquiterpene phytoalexins (Chappell and Nable 1987; Moreau and Preisig 1993; Vögeli et al. 1990). However, concomitant with the redistribution of the NbEAS to the ER (Fig. 1), expression of MmFIT2 induced the accumulation of capsidiol by over 200% relative to the P19 expression alone (Fig. 4), suggesting that the MmFIT2-dependent re-localization of NbEAS could help to accumulate more sesquiterpenes. Expression of MmDGAT2



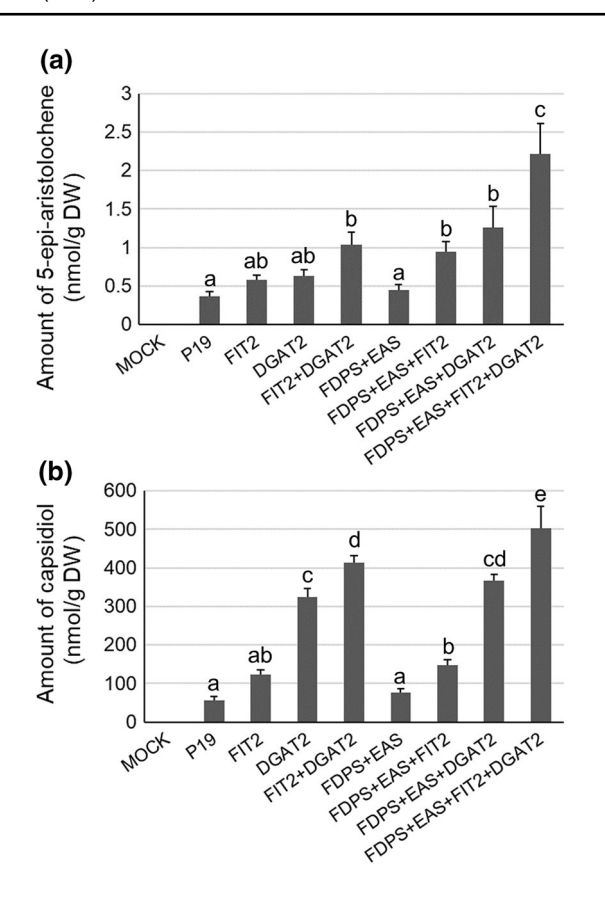


Fig. 4 Expression of MmFIT2 and MmDGAT2 promotes accumulation of sesquiterpenes in N. benthamiana leaves. Shown are contents of 5-epi-aristolochene (a) and capsidiol (b) in N. benthamiana leaves (co)expressing the indicated coding sequence(s). Values are averages and SD of three biological replicates. Different letters on top of the bars indicate significant difference at P < 0.05 determined by one-way ANOVA followed by Tukey's post-test

in *N. benthamiana* leaves led to a twofold increase in 5-epiaristolochene as well as a sixfold increase in capsidiol, and combined expression of MmDGAT2 and MmFIT2 further elevated the content of 5-epi-aristolochene and capsidiol to 1 and 414 nmol per gram dry weight, respectively (Fig. 4). The marked increases in sesquiterpene accumulation by expressing both MmFIT2 and MmDGAT2 suggest that directing the formation of a hydrophobic compartment in plant cells offers an efficient platform for the synthesis and accumulation of sesquiterpenes.

Over-expression of avian FDPS in combination with NbEAS in *N. benthamiana* leaves (to provide additional substrate for the sesquiterpene synthase; Jiang et al. 2016; Wu et al. 2006), did not lead to additional accumulation of 5-epi-aristolochene or capsidiol over the amounts generated by endogenous enzymes in the P19-only transformed cells (Fig. 4), suggesting that the accumulation of additional sesquiterpenes might be normally constrained by the limited storage capacity in leaf cells. *Agrobacterium* infiltration with MmFIT2 and/or MmDGAT2 in leaves overexpressing

FDPS and NbEAS greatly increased the content of 5-epiaristolochene and capsidiol in a trend similar to previous measurements in leaves without ectopic expression of FDPS and NbEAS (Fig. 4). In fact, the most dramatic increase of 5-epi-aristolochene (sevenfold) and capsidiol (tenfold) in N. benthamiana leaves was achieved by combined expression of FDPS, NbEAS, MmFIT2, and MmDGAT2 (Fig. 4). Expression of transgenes in Agrobacterium-infiltrated N. benthamiana leaves was verified by RT-PCR (Supplemental Fig. 6). Collectively, these data indicate that the accumulation of sesquiterpenes in plant vegetative tissues can be promoted by providing excessive neutral lipids (i.e., TAGs) and more hydrophobic compartments for sesquiterpene storage. Hence, MmFIT2, due to its ability to promote the biogenesis of LDs, supports an enhanced accumulation of sesquiterpenes.

Discussion

Mouse FIT2 functions in plant cells to promote LD biogenesis in a manner similar to that in mammalian cells, whereby FIT2 binds to TAGs synthesized between the ER bilayer and modulates ER lipid composition at the sites of LD formation (Cai et al. 2017; Choudhary et al. 2018; Gross et al. 2010; Kadereit et al. 2008). The functional activity of MmFIT2 in a plant cell context suggests that MmFIT2 may interact with some native plant protein machinery involved in LD biogenesis. Indeed, the affinity-capture assay using transiently expressed GFP-MmFIT2 in N. benthamiana pulled-down ER-resident proteins involved in glycerolipid biosynthesis (i.e., LPCAT, GPAT) as well as proteins related to ER membrane-shaping (i.e., reticulons), which likely cooperate with MmFIT2 to reorganize the ER for LD emergence (Supplemental Table 2; Choudhary et al. 2018; Li-Beisson et al. 2010; Sparkes et al. 2010). However, we were surprised to find proteins related to terpene biosynthesis in a considerably high abundance in the MmFIT2 pull-down list (Table 1) given the lack of a previous connection between terpene biosynthesis and TAG/LD formation. It was unlikely that the reproducible association of MmFIT2 in membranes with terpene biosynthesis proteins was an artifact of the pull-down assay, since no NbEAS or other terpene biosynthetic machinery was found in GFPonly precipitation experiments. Nevertheless, these results were tested further using an alternative approach, whereby the subcellular location of NbEAS (and AtTPS21) was visualized in planta by confocal laser scanning fluorescence microscopy.

NbEAS is a functionally soluble, cytoplasmic sesquiterpene synthase that catalyzes the rate limiting step in capsidiol biosynthesis (Facchini and Chappell 1992). By both the affinity-capture experiments (Table 1), and



confocal microscopy (Figs. 1, 2), expression of MmFIT2 supported a redistribution of NbEAS at the subcellular level. The MmFIT2-dependent re-localization of NbEAS may be a result of a direct interaction between MmFIT2 and NbEAS, or, perhaps more likely, an indirect interaction through MmFIT2-recruited proteins at the LD budding sites that interact with NbEAS. It is possible that MmFIT2 sequesters membrane-bound proteins to the ER sites of LD formation, and these membrane proteins may interact with NbEAS to bring it to the cytoplasmic face of the ER. In any case, this MmFIT2- dependent redistribution of terpene synthesis machinery resulted in increased LD formation and an increase in storage TAGs as well as sesquiterpenes. The formation of a hydrophobic compartment alone, by expression of MmDGAT2, was sufficient to elevate substantially the amount of sesquiterpene accumulation, indicating that at least part of this phenomenon likely was afforded by the close proximity to a hydrophobic compartment and a neutral lipid co-solvent. However, expression of MmFIT2 on its own or with MmDGAT2, stimulated the further accumulation of sesquiterpenes suggesting that a functional association of NbEAS with a subcellular region involved in the biogenesis and packaging of lipid droplets enhanced the efficiency with which sesquiterpenes can be compartmentalized in plant cells. Recently, it was shown that the sesquiterpene, bisabolol, can be substantially elevated in plant tissues by the co-expression of WRINKLED1, DGAT1, and oleosin1, and that this was due to its accumulation of cytoplasmic lipid droplets (Delatte et al. 2018). Similarly, here we observed a marked increase in the amounts of sesquiterpenes (5-epiaristolochene and capsidiol) when mouse DGAT2 was expressed in N. benthamiana leaves to promote TAG assembly (Figs. 3, 4). In addition, however, using the MmFIT2 represents a novel approach to influence the biogenesis of the LD compartment for the co-packaging of terpenes and other neutral lipids. Unlike DGAT which synthesizes TAG, MmFIT2 does not synthesize TAG, but rather binds to TAG and supports the partitioning of neutral lipids into LDs (Gross et al. 2011). One possibility is that the MmFIT2dependent redistribution of enzymes for sesquiterpene biosynthesis at the LD-forming domains couples the sesquiterpene biosynthesis with the LD biogenesis machinery, which increases the efficiency of partitioning sesquiterpenes into LDs. Although perhaps less likely, it is also possible that the re-localization of NbEAS, and perhaps FDPS, sequesters FPP, 5-epi-aristolochene and capsidiol from the cytoplasmic MVA pathway, which may attenuate any feedback downregulation of carbon flux through MVA pathway and thereby increase accumulation of sesquiterpenes (Gardner and Hampton 1999). In any case, the subcellular redistribution of sesquiterpene biosynthesis supported by the MmFIT2 provides an efficient means of elevating cytoplasmic levels of high-value sesquiterpenes in plant cells. Co-expression of lipogenic proteins with sesquiterpene synthetic machinery represents a novel strategy to promote co-accumulation of neutral lipids and sesquiterpenes. Stable transformation using the gene combinations tested in the transient expression system would be the necessary next step to engineer sesquiterpene accumulation in plant cells.

Figure 5 provides a hypothetical model of the postulated participation of MmFIT2 and MmDGAT2 in re-localizing NbEAS and promoting capsidiol accumulation in plant cells. MmFIT2 recruits NbEAS from cytoplasm to an ER region where neutral lipids accumulate and LD biogenesis is initiated. This action at specific regions of the ER membrane enhances the coordination of sesquiterpene biosynthesis and the partitioning of sesquiterpenes into LDs. MmDGAT2, on the other hand, does not recruit NbEAS but rather promotes the assembly of TAG, which serves as a co-solvent for the hydrophobic sesquiterpene and leads to marked increase in sesquiterpene content. When MmFIT2 and MmDGAT2 are co-expressed in plant cells, MmFIT2 somehow recruits NbEAS to the ER sites of LD formation where MmDGAT2 synthesizes excessive amount of TAG to dissolve sesquiterpene, providing an optimized subcellular environment for sesquiterpene synthesis, packaging and storage. It is not clear at this stage what mediates the interaction of EAS with MmFIT2, although it is unlikely to be through a direct interaction, since MmFIT2 it a non-native protein, and there are no obvious plant homologues for FIT2. Despite the inclusion of non-ionic detergent in the pull-down assays, many proteins were present in the MmFIT2-specific pull-downs, and NbEAS may interact with one of them in a large complex. There may be some type of scaffold protein that is recruited to this region of the ER to support neutral lipid packaging, and this also may provide a specific location in the ER for EAS interaction. Further work is required to determine the precise mechanisms that recruit NbEAS to the MmFIT2induced ER subdomains, but two approaches confirmed this phenomenon and this re-localization was demonstrated for two different terpene synthases. Moreover, the interactions, whether direct or indirect, supported a substantial accumulation of capsidiol, indicating that the interactions produced a functional complex for efficient terpenoid synthesis.

One well-established strategy for engineering neutral glycerolipids in plant vegetative tissues has been described as "push, pull, package, and protect" strategy (Pyc et al. 2017b; Vanhercke et al. 2014; Xu and Shanklin 2016). In this approach, fatty acid synthesis is induced by seed-specific transcription factors (i.e., LEC2 and WRINKL1) to "push" carbon flux into lipid biosynthesis, the DGAT enzyme promotes TAG assembly to "pull" fatty acids to TAGs, proteins responsible for LD budding from the ER (i.e., SEIPIN and FIT2) enhance lipid compartmentalization to "package" neutral lipids synthesized between the ER bilayer into LDs, and finally LD coat proteins (i.e., oleosins)



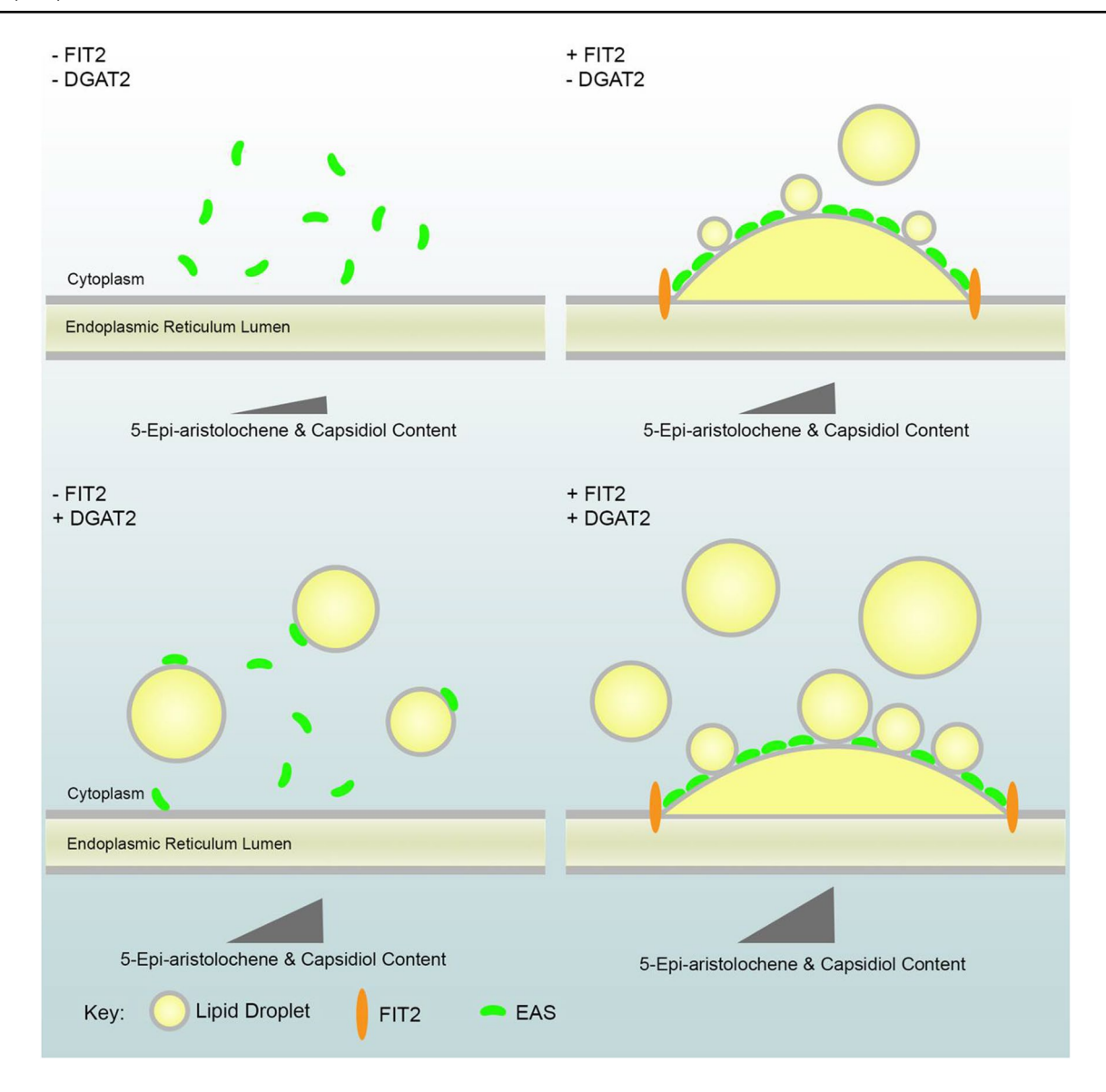


Fig. 5 Proposed hypothetical model for MmFIT2 and MmDGAT2 in promoting the subcellular redistribution of NbEAS (or AtTPS21) and promoting sesquiterpene accumulation in plant cells. MmFIT2 promotes the re-location of NbEAS from the cytoplasm to ER subdomains responsible for LD formation, and elevates the contents of 5-epi-aristolochene and capsidiol probably through partitioning sesquiterpenes into LDs. When co-expressed with MmDGAT2 alone,

NbEAS mostly localizes to the cytoplasm and occasionally associates with cytoplasmic LDs. MmDGAT2 expression increases the contents of 5-epi-aristolochene and capsidiol, which can be further enhanced by co-expressing MmFIT2 and MmDGAT2. Gray triangles, depict the relative changes in sesquiterpene contents under the designated conditions

cover the LD surface and "protect" the enclosed neutral lipid from turnover. According to our results here and those of others, we propose a similar strategy for engineering terpenes in plant vegetative tissues. Expression of heterologous pathway enzymes (i.e., avian FDPS and truncated HMGR) that are not subject to the regulatory mechanism in plant cells could "push" photosynthetic carbon into terpene synthesis (Reed et al. 2017; Wu et al. 2006). Various downstream terpene synthases (i.e., botryococcene synthase, patchoulol synthase, or EAS) could be introduced to "pull" carbon from isoprenoid precursors into desired terpenes

(Jiang et al. 2016; Wu et al. 2006). Then, lipogenic proteins (i.e., FIT2, SEIPIN, LDAP, LDIP, and DGAT) help to "package" terpenes into LDs (Cai et al. 2015; Delatte et al. 2018; Gidda et al. 2016; Pyc et al. 2017a). This "packaging" step may also be achieved by fusing a LD-targeting domain (i.e., oleosin hydrophobic domain) to the terpene synthase to redirect the terpene synthesis into LDs (Zhao et al. 2018). Finally, the terpenes packaged into LDs are likely isolated from the active metabolic regulation and, therefore, are "protected" from turnover (Gershenzon et al. 1993). Taken together, the mammalian lipogenic protein factors, MmFIT2



and MmDGAT2, described by our studies provide novel components to include in the efforts to engineer the accumulation of valuable terpenes in plant vegetative tissues.

Author contribution statement YC performed experiments. All authors conceived and designed experiments, interpreted and evaluated data, and contributed to the writing of the article.

Acknowledgements This research was initiated as part of a classroom undergraduate research course, BIOL 3900, at UNT with the support of the National Science Foundation (NSF), Integrative Organismal Systems Division (IOS-1656263). Course instructors and students deserving special recognition include Dr. Ashley Cannon, Charles Anderson, Rachael Tumer, Selina Aguilar, Matthew Barker, Andre Castaneda, Jessica Cruz, Nelson Duarte, Palamandadige Fernando, Gretchen Johnson, Bilal Khoncarly, Jose Lopez, Catherine Stout, Pratheeba Thirucenthilvelan. In addition, the contributions of the spring 2017 undergraduate biochemistry laboratory at Bethel University (St. Paul, MN) directed by Dr. Angela Stoeckman, are gratefully acknowledged. The expansion of this research was supported by the US Department of Energy (DOE) Office of Science, BES-Physical Biosciences program (DE-SC0016536). We are grateful to Dr. Qing Liu (CSIRO Plant Industry) for providing the construct pORE04-P19, Dr. David Silver (Duke—National University of Singapore) for providing the construct with MmFIT2 coding sequence, Dr. Mina Aziz for assistance with GC-MS, and Douglas Whitten (Michigan State University Proteomics Core Facility) for carrying out the proteomics analysis.

References

- Bohlmann J, Keeling CI (2008) Terpenoid biomaterials. Plant J 54(4):656–669. https://doi.org/10.1111/j.1365-313X.2008.03449 .x
- Brown GD (2010) The biosynthesis of artemisinin (Qinghaosu) and the phytochemistry of *Artemisia annua* L. (Qinghao). Molecules 15(11):7603–7698. https://doi.org/10.3390/molecules15117603
- Brückner K, Tissier A (2013) High-level diterpene production by transient expression in *Nicotiana benthamiana*. Plant Methods 9(1):46. https://doi.org/10.1186/1746-4811-9-46
- Cai Y, Goodman JM, Pyc M, Mullen RT, Dyer JM, Chapman KD (2015) Arabidopsis SEIPIN proteins modulate triacylglycerol accumulation and influence lipid droplet proliferation. Plant Cell 27(9):2616–2636. https://doi.org/10.1105/tpc.15.00588
- Cai Y, McClinchie E, Price A, Nguyen TN, Gidda SK, Watt SC, Yurchenko O, Park S, Sturtevant D, Mullen RT, Dyer JM, Chapman KD (2017) Mouse fat storage-inducing transmembrane protein 2 (FIT2) promotes lipid droplet accumulation in plants. Plant Biotechnol J 15(7):824–836. https://doi.org/10.1111/pbi.12678
- Chapman KD, Dyer JM, Mullen RT (2012) Biogenesis and functions of lipid droplets in plants. J Lipid Res 53(2):215–226. https://doi.org/10.1194/jlr.R021436
- Chappell J, Nable R (1987) Induction of sesquiterpenoid biosynthesis in tobacco cell suspension cultures by fungal elicitor. Plant Physiol 85(2):469–473
- Choudhary V, Ojha N, Golden A, Prinz WA (2015) A conserved family of proteins facilitates nascent lipid droplet budding from the ER. J Cell Biol 211(2):261–271. https://doi.org/10.1083/jcb.201505067
- Choudhary V, Golani G, Joshi AS, Cottier S, Schneiter R, Prinz WA, Kozlov MM (2018) Architecture of lipid droplets in

- endoplasmic reticulum is determined by phospholipid intrinsic curvature. Curr Biol 28(6):915–926. https://doi.org/10.1016/j.cub.2018.02.020
- Crouzet J, Roland J, Peeters E, Trombik T, Ducos E, Nader J, Boutry M (2013) NtPDR1, a plasma membrane ABC transporter from *Nicotiana tabacum*, is involved in diterpene transport. Plant Mol Biol 82(1–2):181–192. https://doi.org/10.1007/s11103-013-0053-0
- Delatte TL, Scaiola G, Molenaar J, de Sousa Farias K, Alves Gomes Albertti L, Busscher J, Verstappen F, Carollo C, Bouwmeester H, Beekwilder J (2018) Engineering storage capacity for volatile sesquiterpenes in *Nicotiana benthamiana* leaves. Plant Biotechnol J. https://doi.org/10.1111/pbi.12933
- Facchini PJ, Chappell J (1992) Gene family for an elicitor-induced sesquiterpene cyclase in tobacco. Proc Natl Acad Sci USA 89(22):11088–11092
- Gardner RG, Hampton RY (1999) A highly conserved signal controls degradation of 3-hydroxy-3-methylglutaryl-coenzyme A (HMG-CoA) reductase in eukaryotes. J Biol Chem 274(44):31671–31678
- Geng S-L, Cui Z-X, Shu B, Zhao S, Yu X-H (2012) Histochemistry and cell wall specialization of oil cells related to the essential oil accumulation in the bark of *Cinnamomum cassia* Presl. (Lauraceae). Plant Prod Sci 15(1):1–9
- Gershenzon J, Murtagh GJ, Croteau R (1993) Absence of rapid terpene turnover in several diverse species of terpene-accumulating plants. Oecologia 96(4):583–592. https://doi.org/10.1007/BF00320517
- Gidda SK, Park S, Pyc M, Yurchenko O, Cai Y, Wu P, Andrews DW, Chapman KD, Dyer JM, Mullen RT (2016) Lipid droplet-associated proteins (LDAPs) are required for the dynamic regulation of neutral lipid compartmentation in plant cells. Plant Physiol 170(4):2052–2071. https://doi.org/10.1104/pp.15.01977
- Gross DA, Snapp EL, Silver DL (2010) Structural insights into triglyceride storage mediated by fat storage-inducing transmembrane (FIT) protein 2. PLoS One 5(5):e10796. https://doi.org/10.1371/journal.pone.0010796
- Gross DA, Zhan C, Silver DL (2011) Direct binding of triglyceride to fat storage-inducing transmembrane proteins 1 and 2 is important for lipid droplet formation. Proc Natl Acad Sci USA 108(49):19581–19586. https://doi.org/10.1073/pnas.1110817108
- Hasegawa M, Mitsuhara I, Seo S, Imai T, Koga J, Okada K, Yamane H, Ohashi Y (2010) Phytoalexin accumulation in the interaction between rice and the blast fungus. Mol Plant Microbe Interact 23(8):1000–1011. https://doi.org/10.1094/MPMI-23-8-1000
- Hemmerlin A, Hoeffler JF, Meyer O, Tritsch D, Kagan IA, Grosdemange-Billiard C, Rohmer M, Bach TJ (2003) Cross-talk between the cytosolic mevalonate and the plastidial methylerythritol phosphate pathways in tobacco bright yellow-2 cells. J Biol Chem 278(29):26666–26676. https://doi.org/10.1074/jbc.M302526200
- Horn PJ, Chapman KD (2014) Metabolite Imager: customized spatial analysis of metabolite distributions in mass spectrometry imaging. Metabolomics 10(2):337–348. https://doi.org/10.1007/s11306-013-0575-0
- Jasiński M, Stukkens Y, Degand H, Purnelle B, Marchand-Brynaert J, Boutry M (2001) A plant plasma membrane ATP binding cassette-type transporter is involved in antifungal terpenoid secretion. Plant Cell 13(5):1095–1107
- Jiang Z, Kempinski C, Bush CJ, Nybo SE, Chappell J (2016) Engineering triterpene and methylated triterpene production in plants provides biochemical and physiological insights into terpene metabolism. Plant Physiol 170(2):702–716. https://doi.org/10.1104/pp.15.01548
- Kadereit B, Kumar P, Wang WJ, Miranda D, Snapp EL, Severina N, Torregroza I, Evans T, Silver DL (2008) Evolutionarily conserved gene family important for fat storage. Proc Natl Acad Sci USA 105(1):94–99. https://doi.org/10.1073/pnas.0708579105
- Kappers IF, Aharoni A, van Herpen TW, Luckerhoff LL, Dicke M, Bouwmeester HJ (2005) Genetic engineering of terpenoid metabolism



attracts bodyguards to Arabidopsis. Science 309(5743):2070–2072. https://doi.org/10.1126/science.1116232

- Kempinski C, Chappell J (2018) Engineering triterpene metabolism in the oilseed of *Arabidopsis thaliana*. Plant Biotechnol J. https://doi.org/10.1111/pbi.12984
- Kempinski C, Jiang Z, Zinck G, Sato SJ, Ge Z, Clemente TE, Chappell J (2018) Engineering linear, branched-chain triterpene metabolism in monocots. Plant Biotechnol J. https://doi.org/10.1111/pbi.12983
- Lange BM (2015) The evolution of plant secretory structures and emergence of terpenoid chemical diversity. Annu Rev Plant Biol 66:139–159. https://doi.org/10.1146/annurev-arplant-043014-114639
- Lange BM, Ahkami A (2013) Metabolic engineering of plant monoterpenes, sesquiterpenes and diterpenes—current status and future opportunities. Plant Biotechnol J 11(2):169–196. https://doi. org/10.1111/pbi.12022
- Li-Beisson Y, Shorrosh B, Beisson F, Andersson MX, Arondel V, Bates PD, Baud S, Bird D, Debono A, Durrett TP, Franke RB, Graham IA, Katayama K, Kelly AA, Larson T, Markham JE, Miquel M, Molina I, Nishida I, Rowland O, Samuels L, Schmid KM, Wada H, Welti R, Xu C, Zallot R, Ohlrogge J (2010) Acyl-lipid metabolism. Arabidopsis Book 8:e0133. https://doi.org/10.1199/tab.0133
- Maldonado-Bonilla LD, Betancourt-Jiménez M, Lozoya-Gloria E (2008) Local and systemic gene expression of sesquiterpene phytoalexin biosynthetic enzymes in plant leaves. Eur J Plant Pathol 121(4):439–449. https://doi.org/10.1007/s10658-007-9262-1
- Moreau RA, Preisig CL (1993) Lipid changes in tobacco cell suspensions following treatment with cellulase elicitor. Physiol Plant 87(1):7–13. https://doi.org/10.1111/j.1399-3054.1993.tb08783.x
- Murashige T, Skoog F (1962) A revised medium for rapid growth and bio assays with tobacco tissue cultures. Physiol Plant 15(3):473–497. https://doi.org/10.1111/j.1399-3054.1962.tb08052.x
- Murphy DJ (2001) The biogenesis and functions of lipid bodies in animals, plants and microorganisms. Prog Lipid Res 40(5):325–438
- Petrie JR, Shrestha P, Liu Q, Mansour MP, Wood CC, Zhou XR, Nichols PD, Green AG, Singh SP (2010) Rapid expression of transgenes driven by seed-specific constructs in leaf tissue: DHA production. Plant Methods 6:8. https://doi. org/10.1186/1746-4811-6-8
- Pyc M, Cai Y, Gidda SK, Yurchenko O, Park S, Kretzschmar FK, Ischebeck T, Valerius O, Braus GH, Chapman KD, Dyer JM, Mullen RT (2017a) Arabidopsis lipid droplet-associated protein (LDAP)—interacting protein (LDIP) influences lipid droplet size and neutral lipid homeostasis in both leaves and seeds. Plant J 92(6):1182–1201. https://doi.org/10.1111/tpj.13754
- Pyc M, Cai Y, Greer MS, Yurchenko O, Chapman KD, Dyer JM, Mullen RT (2017b) Turning over a new leaf in lipid droplet biology. Trends Plant Sci 22(7):596–609. https://doi.org/10.1016/j.tplants.2017.03.012
- Ralston L, Kwon ST, Schoenbeck M, Ralston J, Schenk DJ, Coates RM, Chappell J (2001) Cloning, heterologous expression, and functional characterization of 5-epi-aristolochene-1,3-dihydroxylase from tobacco (*Nicotiana tabacum*). Arch Biochem Biophys 393(2):222–235. https://doi.org/10.1006/abbi.2001.2483
- Reed J, Stephenson MJ, Miettinen K, Brouwer B, Leveau A, Brett P, Goss RJM, Goossens A, O'Connell MA, Osbourn A (2017) A translational synthetic biology platform for rapid access to gram-scale quantities of novel drug-like molecules. Metab Eng 42:185–193. https://doi.org/10.1016/j.ymben.2017.06.012
- Reiling KK, Yoshikuni Y, Martin VJ, Newman J, Bohlmann J, Keasling JD (2004) Mono and diterpene production in *Escherichia coli*. Biotechnol Bioeng 87(2):200–212. https://doi.org/10.1002/bit.20128
- Ro DK, Paradise EM, Ouellet M, Fisher KJ, Newman KL, Ndungu JM, Ho KA, Eachus RA, Ham TS, Kirby J, Chang MC, Withers

- ST, Shiba Y, Sarpong R, Keasling JD (2006) Production of the antimalarial drug precursor artemisinic acid in engineered yeast. Nature 440(7086):940–943. https://doi.org/10.1038/nature04640
- Sallaud C, Giacalone C, Töpfer R, Goepfert S, Bakaher N, Rösti S, Tissier A (2012) Characterization of two genes for the biosynthesis of the labdane diterpene Z-abienol in tobacco (*Nicotiana tabacum*) glandular trichomes. Plant J 72(1):1–17. https://doi.org/10.1111/j.1365-313X.2012.05068.x
- Sasabe M, Toyoda K, Shiraishi T, Inagaki Y, Ichinose Y (2002) cDNA cloning and characterization of tobacco ABC transporter: NtPDR1 is a novel elicitor-responsive gene. FEBS Lett 518(1–3):164–168
- Schwab W, Davidovich-Rikanati R, Lewinsohn E (2008) Biosynthesis of plant-derived flavor compounds. Plant J 54(4):712–732. https://doi.org/10.1111/j.1365-313X.2008.03446.x
- Shevchenko A, Wilm M, Vorm O, Mann M (1996) Mass spectrometric sequencing of proteins silver-stained polyacrylamide gels. Anal Chem 68(5):850–858
- Shimada TL, Takano Y, Shimada T, Fujiwara M, Fukao Y, Mori M, Okazaki Y, Saito K, Sasaki R, Aoki K, Hara-Nishimura I (2014) Leaf oil body functions as a subcellular factory for the production of a phytoalexin in Arabidopsis. Plant Physiol 164(1):105–118. https://doi.org/10.1104/pp.113.230185
- Sparkes I, Tolley N, Aller I, Svozil J, Osterrieder A, Botchway S, Mueller C, Frigerio L, Hawes C (2010) Five Arabidopsis reticulon isoforms share endoplasmic reticulum location, topology, and membrane-shaping properties. Plant Cell 22(4):1333–1343. https://doi.org/10.1105/tpc.110.074385
- Starks CM, Back K, Chappell J, Noel JP (1997) Structural basis for cyclic terpene biosynthesis by tobacco 5-epi-aristolochene synthase. Science 277(5333):1815–1820
- Takahashi S, Yeo Y, Greenhagen BT, McMullin T, Song L, Maurina-Brunker J, Rosson R, Noel JP, Chappell J (2007) Metabolic engineering of sesquiterpene metabolism in yeast. Biotechnol Bioeng 97(1):170–181. https://doi.org/10.1002/bit.21216
- Tarshis LC, Yan M, Poulter CD, Sacchettini JC (1994) Crystal structure of recombinant farnesyl diphosphate synthase at 2.6-A resolution. Biochemistry 33(36):10871–10877
- Tholl D, Lee S (2011) Terpene specialized metabolism in *Arabidopsis thaliana*. Arabidopsis Book 9:e0143. https://doi.org/10.1199/tab.0143
- Vanhercke T, El Tahchy A, Liu Q, Zhou XR, Shrestha P, Divi UK, Ral JP, Mansour MP, Nichols PD, James CN, Horn PJ, Chapman KD, Beaudoin F, Ruiz-López N, Larkin PJ, de Feyter RC, Singh SP, Petrie JR (2014) Metabolic engineering of biomass for high energy density: oilseed-like triacylglycerol yields from plant leaves. Plant Biotechnol J 12(2):231–239. https://doi.org/10.1111/ pbi.12131
- Vögeli U, Freeman JW, Chappell J (1990) Purification and characterization of an inducible sesquiterpene cyclase from elicitor-treated tobacco cell suspension cultures. Plant Physiol 93(1):182–187
- Wang B, Kashkooli AB, Sallets A, Ting HM, de Ruijter NCA, Olofsson L, Brodelius P, Pottier M, Boutry M, Bouwmeester H, van der Krol AR (2016) Transient production of artemisinin in *Nicotiana benthamiana* is boosted by a specific lipid transfer protein from A. annua. Metab Eng 38:159–169. https://doi.org/10.1016/j.ymben.2016.07.004
- Whitehead IM, Threlfall DR, Ewing DF (1989) 5-epi-aristolochene is a common precursor of the sesquiterpenoid phytoalexins capsidiol and debneyol. Phytochemistry 28(3):775–779
- Wilfling F, Haas JT, Walther TC, Farese RV (2014) Lipid droplet biogenesis. Curr Opin Cell Biol 29:39–45. https://doi.org/10.1016/j.ceb.2014.03.008
- Wu S, Schalk M, Clark A, Miles RB, Coates R, Chappell J (2006) Redirection of cytosolic or plastidic isoprenoid precursors elevates terpene production in plants. Nat Biotechnol 24:1441



- Wu S, Jiang Z, Kempinski C, Eric Nybo S, Husodo S, Williams R, Chappell J (2012) Engineering triterpene metabolism in tobacco. Planta 236(3):867–877. https://doi.org/10.1007/s00425-012-1680-4
- Xu C, Shanklin J (2016) Triacylglycerol metabolism, function, and accumulation in plant vegetative tissues. Annu Rev Plant Biol 67:179–206. https://doi.org/10.1146/annurev-arplant-04301 5-111641
- Yen CL, Stone SJ, Koliwad S, Harris C, Farese RV (2008) Thematic review series: glycerolipids. DGAT enzymes and triacylglycerol biosynthesis. J Lipid Res 49(11):2283–2301. https://doi.org/10.1194/jlr.r800018-jlr200
- Yurchenko O, Shockey JM, Gidda SK, Silver MI, Chapman KD, Mullen RT, Dyer JM (2017) Engineering the production of conjugated fatty acids in *Arabidopsis thaliana* leaves. Plant Biotechnol J 15(8):1010–1023. https://doi.org/10.1111/pbi.12695

- Zhao C, Kim Y, Zeng Y, Li M, Wang X, Hu C, Gorman C, Dai SY, Ding SY, Yuan JS (2018) Co-compartmentation of terpene biosynthesis and storage via synthetic droplet. ACS Synth Biol 7(3):774–781. https://doi.org/10.1021/acssynbio.7b00368
- Zhuang X, Chappell J (2015) Building terpene production platforms in yeast. Biotechnol Bioeng 112(9):1854–1864. https://doi.org/10.1002/bit.25588

Publisher's Note Springer Nature remains neutral with regard to jurisdictional claims in published maps and institutional affiliations.

